물리탐사
Vol. 5, No. 4, 2002, p. 316~322

A Fast Inversion Method for Interpreting Single-Hole Electromagnetic Data

Hee Joon Kim[1] and Jung Mo Lee[2]

단일 시추공 전자탐사 자료 해석을 위한 빠른 역산법

김희준[1] · 이정모[2]

Abstract : A computationally efficient inversion scheme has been developed using the extended Born or localized nonlinear approximation to analyze electromagnetic fields obtained in a single-hole environment. The medium is assumed to be cylindrically symmetric about the borehole, and to maintain the symmetry vertical magnetic dipole source is used throughout. The efficiency and robustness of an inversion scheme is very much dependent on the proper use of Lagrange multiplier, which is often provided manually to achieve desired convergence. In this study, an automatic Lagrange multiplier selection scheme has been developed to enhance the utility of the inversion scheme in handling field data. The inversion scheme has been tested using synthetic data to show its stability and effectiveness.

Keywords : single-hole, localized nonlinear approximation, cylindrical symmetry, inversion

요 약 : 단일 시추공 환경에서 얻어지는 전자기장을 해석하기 위해 확장 Born 혹은 국소비선형 근사를 이용한 계산시간이 짧고 효율적인 역산법을 만들었다. 매질은 시추공에 관해 축대칭이라 가정하였으며 그 대칭성을 유지하기 위해 수직 자기 쌍극자원을 사용하였다. 역산법의 효율성과 안정성은 적절한 라그랑지계수의 사용에 크게 의존하지만 이는 일반적으로 원하는 수렴성을 달성하기 위해 수작업으로 결정된다. 본 연구에서는 현장 자료를 다루는 역산법의 효율을 향상하기 위해 라그랑지계수의 자동결정법을 개발하였다. 그 역산법의 안정성과 효율성은 이론모델링 자료를 사용하여 검토되었다.

주요어 : 단일 시추공, 국소비선형 근사, 축대칭, 역산법

Introduction

High-resolution imaging of electrical conductivity has been the subject of many studies in cross-hole tomography using electromagnetic (EM) fields (Zhou *et al.*, 1993; Wilt *et al.*, 1995; Alumbaugh and Morrison, 1995; Newman, 1995; Alumbaugh and Newman, 1997). Although the theoretical understanding and associated field practices for cross-hole EM methods are relatively mature, these techniques are costly and sometimes it is difficult to find two adjacent boreholes for cross-hole surveys. The cost can be greatly reduced if a single-hole survey method could be developed.

The main advantage of integral equation (IE) method in comparison with the finite difference (FD) and/or the finite element (FE) methods, is the fast and accurate simulation of compact three-dimensional (3-D) bodies in a layered background (Hohmann, 1975). The FD and FE methods are suitable for modeling EM fields in complex structures with large-scale conductivity variations. In principle, the IE method can handle these models too, but the huge demand on computer resources places a practical limit on its use. This is because of the full matrix arising from the IE formulation.

Another advantage of the IE method over the FD or FE method is its greater suitability for inversion. IE formulation readily contains a sensitivity matrix, which can be revised at each inversion iteration at little expense. With FD or FE, in contrast, the sensitivity matrix has to be recomputed at each iteration at a cost nearly equal to that of full forward modeling. The IE method, however, has to overcome severe practical limitations imposed on the numerical size of the anomalous domain for inversion purposes. In this direction,

*2002년 9월 27일 접수
1) 부경대학교 환경탐사공학과(Department of Environmental Exploration Engineering, Pukyong National University)
2) 경북대학교 지질학과(Department of Geology, Kyungpook National University)

several approximate methods such as the localized nonlinear (LN) approximation (Habashy et al., 1993) and quasi-linear approximation (Zhdanov and Fang, 1996) have been developed recently.

In this paper an advantage of the LN approximation is exploited with applications to single-hole inversion of EM data. We begin our discussion with a review of the LN approximation of IE solutions. We then consider its accuracy for a cylindrically symmetric model and describe our inversion algorithm. Finally, we demonstrate the stability and effectiveness of the approach by inverting synthetic data.

LN approximation

Maxwell's equations with an $e^{+i\omega t}$ time dependence, neglecting displacement currents, are written as

$$\nabla \times \mathbf{E}(\mathbf{r}) = -i\omega\mu \mathbf{H}(\mathbf{r}), \tag{1}$$

$$\nabla \times \mathbf{H}(\mathbf{r}) = \sigma(\mathbf{r})\mathbf{E}(\mathbf{r}) + \mathbf{J}_s(\mathbf{r} - \mathbf{r}_s), \tag{2}$$

where $\mathbf{J}_s$ is the impressed current source at $\mathbf{r}_s$. The magnetic permeability μ is assumed to be constant and equal to that of free space. The electrical conductivity σ is heterogeneous and it may be divided into

$$\sigma(\mathbf{r}) = \sigma_b + \Delta\sigma(\mathbf{r}), \tag{3}$$

where the subscript b indicates the background. The conductivity of the background medium is assumed uniform. The differential equation for the electric field is derived from equations (1) and (2) as

$$\nabla \times \nabla \times \mathbf{E}(\mathbf{r}) + i\omega\mu\sigma(\mathbf{r})\mathbf{E}(\mathbf{r}) = -i\omega\mu \mathbf{J}_s(\mathbf{r} - \mathbf{r}_s), \tag{4}$$

and the numerical solution for the electric field may be obtained using either the FE or FD method. Alternatively, numerical solution may be obtained using the IE method involving the Green's function that satisfies

$$\nabla \times \nabla \times \mathbf{G}_E(\mathbf{r} - \mathbf{r}') + i\omega\mu\sigma_b \mathbf{G}_E(\mathbf{r} - \mathbf{r}') = \mathbf{I}\delta(\mathbf{r}' - \mathbf{r}_s), \tag{5}$$

where $\mathbf{I}$ is the identity tensor, and the subscript E signifies that the Green's function translates current source $\mathbf{J}_s$ to electric field $\mathbf{E}$. Each vector component of the Green's tensor $\mathbf{G}_E(\mathbf{r}\text{-}\mathbf{r}')$ is the vector electric field at $\mathbf{r}$ due to a point source at $\mathbf{r}'$ with its current density of $-(i\omega\mu)^{-1}$ A/m^2, polarized in x, y, and z, respectively. Using equations (4) and (5), one can derive an IE solution for the electric field as

$$\mathbf{E}(\mathbf{r}) = \mathbf{E}_b(\mathbf{r}) - i\omega\mu \int_V \mathbf{G}_E(\mathbf{r} - \mathbf{r}') \cdot \Delta\sigma(\mathbf{r}')\mathbf{E}(\mathbf{r}')dv', \tag{6}$$

where $\mathbf{E}_b(\mathbf{r})$ is the background electric field that would exist in the presence of background medium only, and the term $\Delta\sigma\mathbf{E}$ inside the integral is called the scattering current (Hohmann, 1975).

Equation (6) is nonlinear because the electric field inside the integral is a function of the conductivity. To obtain a numerical solution, the anomalous body is divided into a number of cells, and a constant electric field is assigned to each cell. Since Raiche (1974) first formulated a volume 3-D IE method, many numerical solutions have been presented on this subject (Hohmann, 1988). The process involved in the volume IE methods requires computing time proportional to the number of cells used, and it quickly becomes impractical as the size of the inhomogeneity is increased to handle realistic problems.

For some important class of problems the complexity associated with a full 3-D problem can be reduced to something much simpler. A model whose electrical conductivities are cylindrically symmetric in the vicinity of a borehole is such an example. In order to preserve the cylindrical symmetry in the resulting EM fields, a horizontal loop current source or a vertical magnetic dipole may be considered in the borehole. In this case the problem is scalar when formulated using the azimuthal electric field E_φ, and the analogous IE solution is

$$E_\varphi(\mathbf{r}) = E_{\varphi b}(\mathbf{r}) - 2\pi i\omega\mu \iint_{\rho z} G_E(\mathbf{r} - \mathbf{r}')\Delta\sigma(\mathbf{r}')E_\varphi(\mathbf{r}')\rho' d\rho' dz', \tag{7}$$

where

$$\mathbf{r} = \vec{\rho} + \vec{z} \quad \text{and} \quad \mathbf{r}' = \vec{\rho}' + \vec{z}'$$

are the position vectors, and the electric field and Green's function are both scalar. The Green's function is given in the form of a Hankel transform as (p. 219, Ward and Hohmann, 1988)

$$\mathbf{G}_E(\mathbf{r} - \mathbf{r}') = -\frac{1}{4\pi} \int_0^\infty \frac{e^{-u_b|z - z'|}}{u_b} \lambda J_1(\lambda\rho) J_1(\lambda\rho') d\lambda, \tag{8}$$

where

$$u_b = (\lambda^2 + i\omega\mu\sigma_b)^{1/2}.$$

Since measurements are usually made for the magnetic field, equation (7) is reformulated to

$$H_z(\mathbf{r}) = H_{zb}(\mathbf{r}) - 2\pi i\omega\mu \iint_{\rho z} G_H(\mathbf{r} - \mathbf{r}')\Delta\sigma(\mathbf{r}')E_\varphi(\mathbf{r}')\rho' d\rho' dz', \tag{9}$$

where $G_H(\mathbf{r}\text{-}\mathbf{r}')$ translates scattering currents $\Delta\sigma(\mathbf{r}')E_\varphi(\mathbf{r}')$ at $\mathbf{r}'$ to the magnetic field at $\mathbf{r}$.

Using equations (7) through (9), one can obtain an IE solution by first dividing the (ρ, z) cross section into a number of cells, and formulate a system of equations for the electric field using a pulse basis function. Sena and Toksoz (1990) presented a cross-hole inversion study for permittivity and conductivity in cylindrically symmetric medium using high-frequency EM, and Alumbaugh and Morrison (1995) investigated cross-hole EM tomography using an iterative Born approximation.

Borehole access for a geophysical survey in producing fields is very limited. For this reason, an efficient single-hole EM imaging is considered using the LN approximation, which offers an efficient and reasonably accurate electric field solution without solving the full IE solution from equation (7). To do this equation (7) is first reformulated to (Habashy *et al.*, 1993).

$$E_\varphi(\mathbf{r})=E_{\varphi b}(\mathbf{r})-2\pi i\omega\mu E_\varphi(\mathbf{r})\iint_{\rho z} G_E(\mathbf{r}-\mathbf{r}')\Delta\sigma(\mathbf{r}')\rho' d\rho' dz'$$

$$-2\pi i\omega\mu\iint_{\rho z} G_E(\mathbf{r}-\mathbf{r}')\Delta\sigma(\mathbf{r}')[E_\varphi(\mathbf{r}')-E_\varphi(\mathbf{r})]\rho' d\rho' dz',$$

or

$$E_\varphi(\mathbf{r})+2\pi i\omega\mu E_\varphi(\mathbf{r})\iint_{\rho z} G_E(\mathbf{r}-\mathbf{r}')\Delta\sigma(\mathbf{r}')\rho' d\rho' dz'$$

$$=E_{\varphi b}(\mathbf{r})-2\pi i\omega\mu\iint_{\rho z} G_E(\mathbf{r}-\mathbf{r}')\Delta\sigma(\mathbf{r}')\,[E_\varphi(\mathbf{r}')-E_\varphi(\mathbf{r})]\rho' d\rho' dz'.$$

If the electric field is continuous in the vicinity of $\mathbf{r}$, the contribution from the second integral may be small compared with the background electric field. This is because when $\mathbf{r}'$ approaches $\mathbf{r}$, the difference in $[E_\varphi(\mathbf{r}')-E_\varphi(\mathbf{r})]$ is getting smaller, so the scattering current is effectively zero at the singular point. When $\mathbf{r}'$ moves away from $\mathbf{r}$, the contribution is also small because the Green's function falls off rapidly. For the type of problem where there is only the azimuthal electric field, therefore, one can get a good approximation even if the second integral is neglected entirely. As a result, one gets

$$E_\varphi(\mathbf{r})\left[1+2\pi i\omega\mu\iint_{\rho z} G_E(\mathbf{r}-\mathbf{r}')\Delta\sigma(\mathbf{r}')\rho' d\rho' dz'\right]\approx E_{\varphi b}(\mathbf{r}),$$

from which one obtains

$$E_\varphi(\mathbf{r})\approx\gamma(\mathbf{r})E_{\varphi b}(\mathbf{r}), \tag{10}$$

where

$$\gamma(\mathbf{r})=\left[1+2\pi i\omega\mu\iint_{\rho z} G_E(\mathbf{r}-\mathbf{r}')\Delta\sigma(\mathbf{r}')\rho' d\rho' dz'\right]^{-1}.$$

Substituting equation (10) into equation (9) yields an approximate magnetic field solution

$$H_z(\mathbf{r})\approx H_{zb}(\mathbf{r})$$

$$-2\pi i\omega\mu\iint_{\rho z} G_H(\mathbf{r}-\mathbf{r}')\Delta\sigma(\mathbf{r}')\gamma(\mathbf{r}')E_{\varphi b}(\mathbf{r}')\rho' d\rho' dz'. \tag{11}$$

To illustrate the efficiency and usefulness of the LN numerical solution, especially in single-hole application, let us consider a simple model consisting of a conductive ring about a borehole axis in a uniform whole space of 100 ohm-m resistivity. The cross section of the ring is a 3 m by 4 m rectangle as shown in Figure 1. Let us vary the transmitter-receiver offset (a in Figure 1), borehole-to-conductor distance (b in Figure 1), vertical distance between the transmitter and the top of the conductor (c in Figure 1), and the conductivity contrast (σ_2/σ_1) and find out how the LN approximated vertical magnetic field compares with the result obtained from the full FE method (Lee *et al.*, 2002). Unless otherwise indicated the frequency used is 100 kHz throughout.

Figure 2 shows the comparison in secondary vertical magnetic fields between the FE (solid and dashed lines) and LN (symbols) solutions for three different transmitter-receiver separations. The center of the body is chosen as $z=0$, and plots are made at the transmitter-receiver midpoint. The conductivity contrast used is 10, and the borehole-to-conductor distance is 3 m. For all three separations of 4 m, 6 m, and 8 m, the two solutions agree very well. More anomalies can

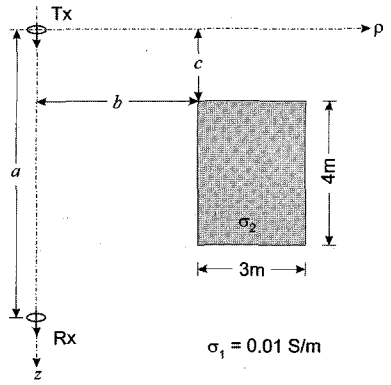

Fig. 1. A cylindrically symmetric model. The inhomogeneous body with a cross-section of 3 m by 4 m is cylindrically symmetric about the borehole in which source and receiver are inserted. The parameters a, b, and c represents the source-receiver, horizontal hole-body and vertical source-body separations, respectively.

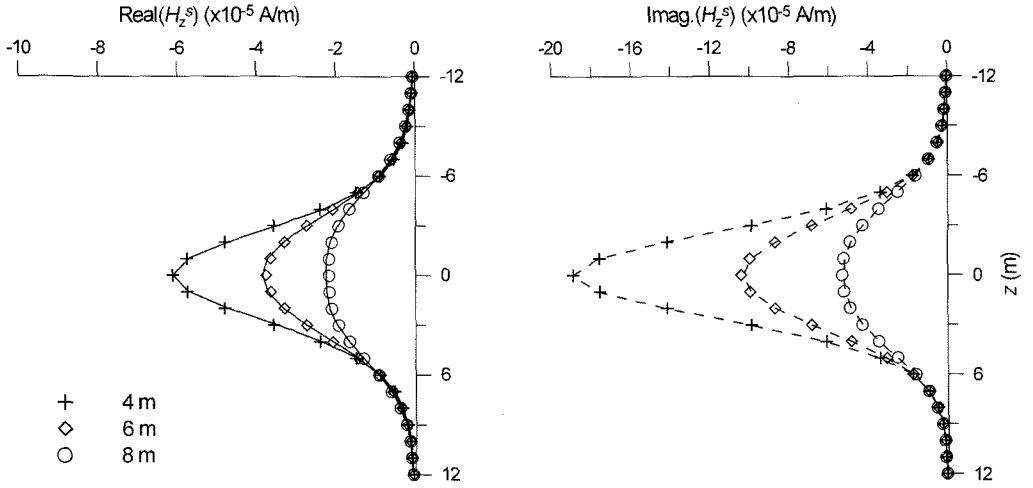

Fig. 2. The effect of source-receiver separation on the vertical component of secondary magnetic fields. Operating frequency is 10^5 Hz. The 0.1 S/m body is located in a whole space of 0.01 S/m at 3 m horizontally away from the borehole.

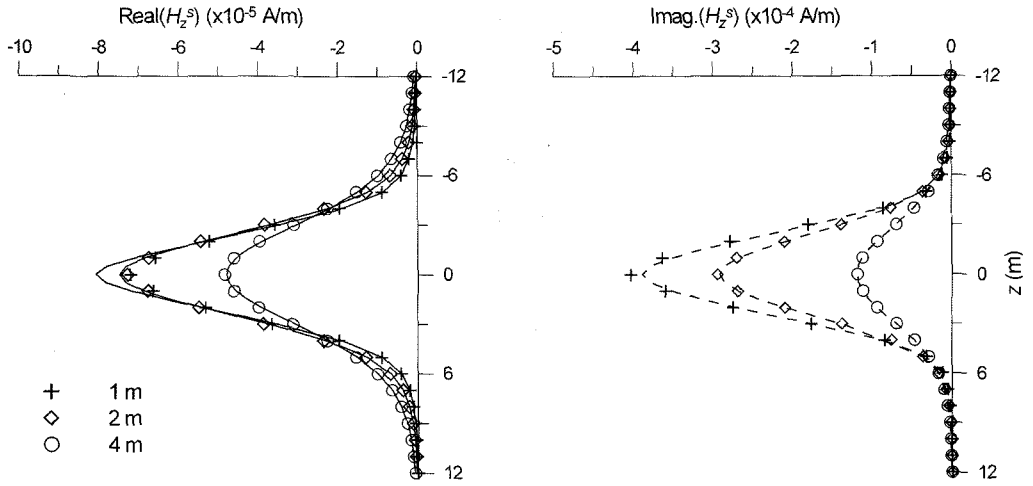

Fig. 3. The effect of hole-body separation on the vertical component of secondary magnetic fields. The operating frequency is 10^5 Hz, the conductivity contrast between body and background is 10, and the source-receiver separation is 4 m.

be observed in the imaginary part. The anomaly also gets stronger for shorter source-receiver separations. At the separation of 4 m the imaginary part of the anomaly is 2.0×10^{-4} A/m, and it is about 8% of the primary field of 2.48×10^{-3} A/m (not shown here).

Next, we consider responses by varying the borehole-to-conductor separation, while the conductivity contrast and transmitter-receiver separation are fixed to 10 and 4 m, respectively. When the separation is small, it is anticipated that the LN approximation may not be as good, because the rapid change in the electric field in the vicinity of the transmitter is not a favorable condition for the LN approximation. Figure 3 confirms this is indeed the case. For the separation of 1 m, one can see significant difference in the peak values of the real part between the FE and LN solutions. The difference is less in the imaginary part.

We are also interested in the quality of the LN solution when the conductivity of the body is increased. The transmitter-receiver separation, borehole-to-conductor distance, and the vertical distance between transmitter and the top of the conductor distance are fixed to 6 m, 3 m, and 4.5 m, respectively. The LN approximation is very well up to the conductivity contrast of 200 as shown in Figure 4. The imaginary part of the LN solution starts deviating from the FE solution beyond the conductivity contrast of 200, while the real part still shows a good agreement.

Finally, the comparison is made for responses in frequency (Figure 5). The conductivity contrast, transmitter-receiver separation, and borehole-to-conductor distance are fixed to 10, 6 m, and 3 m, respectively, and the FE and LN

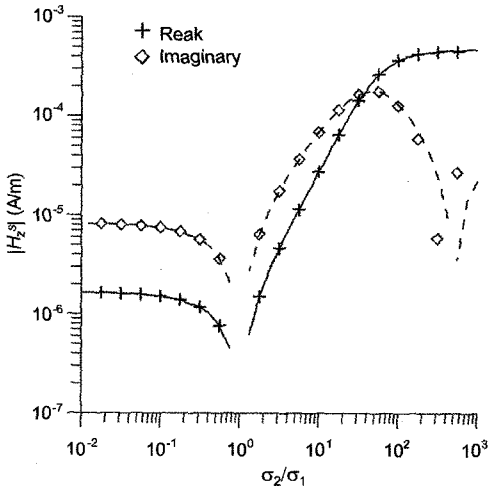

Fig. 4. The effect of conductivity contrast between body and background on the secondary magnetic fields. The operating frequency is 10^5 Hz, the source-receiver separation is 6 m and the horizontal hole-body separation is 3 m.

solutions are obtained for frequencies ranging from 200 Hz to 80 MHz. Two solutions show a good agreement all the way up to 2 MHz (see details on the right of Figure 5).

Inversion

Based on the encouraging results of the LN approximation, we have proceeded to implement the single-hole EM inversion. Measurement positions are in the same borehole as the transmitter, so the radial distance ρ is zero. Upon dividing the inhomogeneity into K elements, the secondary magnetic field at the i-th receiver position in the borehole may be written as

$$H_{zi}^{s} \approx -2\pi i\omega\mu \sum_{k=1}^{K} \Delta\sigma_k \gamma_k E_{\varphi bk} \iint_{S_k} G_H(\rho', z_i - z')\rho' d\rho' dz', \tag{12}$$

where the subscript k denotes the k-th element. The corresponding Green's function for the magnetic field may be deduced from the electric field Green's function (8) as

$$G_H(\rho', z_i - z') = \frac{1}{4\pi i\omega\mu} \int_0^{\infty} \frac{e^{-u_b|z-z'|}}{u_b} \lambda^2 J_1(\lambda\rho') d\lambda. \tag{13}$$

For the inversion, the sensitivity of the magnetic field with respect to the change in conductivity can be easily obtained from equation (12). Taking derivative of the data with respect to the j-th conductivity parameter and neglecting the dependence of γ_j on $\Delta\sigma_j$, the sensitivity becomes

$$\frac{\partial H_{zi}^{s}}{\partial \sigma_j} \approx -2\pi i\omega\mu\gamma_j E_{\varphi bj} \iint_{S_j} G_H(\rho', z_i - z')\rho' d\rho' dz', \tag{14}$$

which can be easily evaluated by integrating over the j-th element.

The inversion procedure starts with the data misfit $\|\mathbf{W}_d[\mathbf{H}(\sigma)-\mathbf{H}_d]\|^2$, where the subscript d denotes data. The data weighting matrix $\mathbf{W}_d$ is used to give relative weights to individual data. If a perturbation $\delta\sigma$ is allowed to the conductivity, the misfit takes a form $\|\mathbf{W}_d[\mathbf{H}(\sigma+\delta\sigma)-\mathbf{H}_d]\|^2$, and the total objective functional may be written as

$$\phi = \|\mathbf{W}_d[\mathbf{H}(\sigma+\delta\sigma)-\mathbf{H}_d]\|^2 + \lambda\|\mathbf{W}_\sigma\delta\sigma\|^2, \tag{15}$$

where the second term on the right-hand side is added to impose a smoothness constraint, and $\mathbf{W}_\sigma$ is a weighting matrix and λ is the Lagrange multiplier that controls the

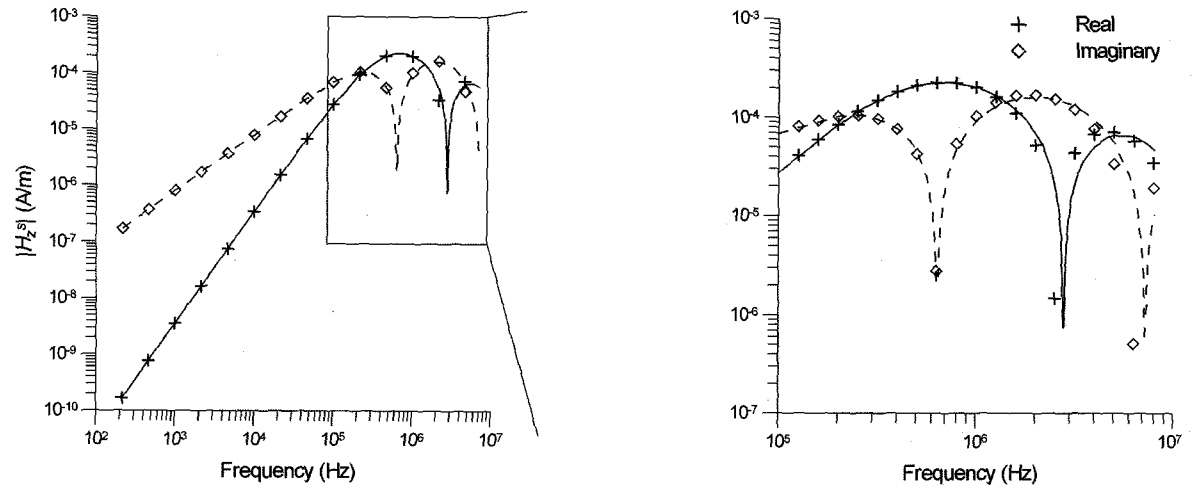

Fig. 5. The effect of operation frequency on the secondary magnetic fields. The source-receiver separation is 6 m. The 0.1 S/m body is located in a whole space of 0.01 S/m at 3 m horizontally away from the borehole.

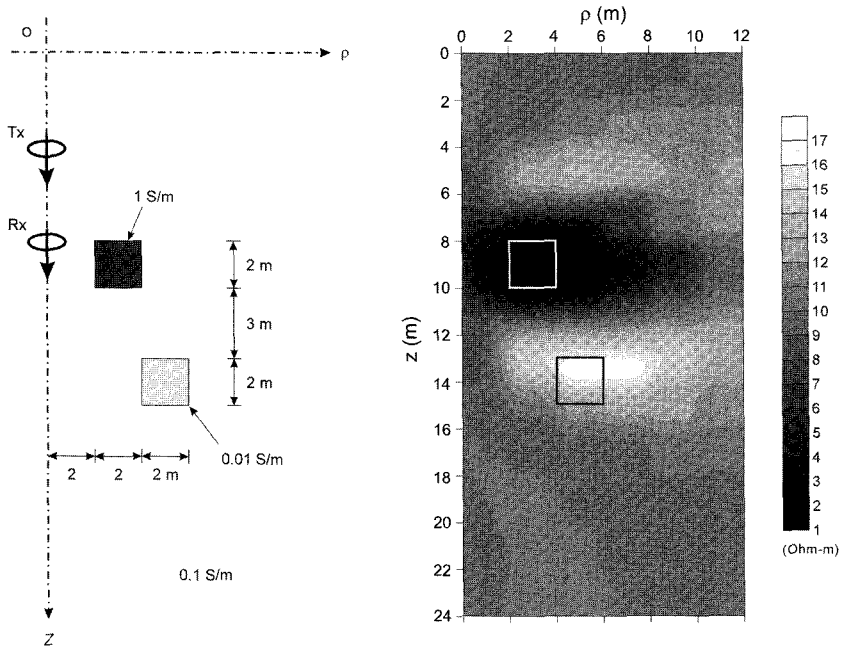

Fig. 6. Inversion of synthetic model. The model (left) used to calculate synthetic data for inversion test consists of two bodies, of 1 S/m and 0.01 S/m, located in a whole-space of 0.1 S/m. An image of two conductors reconstructed from the synthetic data after 8th iteration.

trade-off between data misfit and parameter smoothness. Expanding the misfit in $\delta\sigma$ using the Taylor series, discarding terms higher than the square term, and letting the variation of the functional with respect to $\delta\sigma$ equal to zero, one can obtain a linear system of equations for the perturbation $\delta\sigma$ as

$$(\mathbf{J}^T\mathbf{W}_d^T\mathbf{W}_d\mathbf{J} + \lambda\mathbf{W}_\sigma^T\mathbf{W}_\sigma)\delta\sigma = -\mathbf{J}^T\mathbf{W}_d^T\mathbf{W}_d\{\mathbf{H}(\sigma) - \mathbf{H}_d\}, \quad (16)$$

where the superscript T indicates matrix transpose, and the entries of Jacobian matrix $\mathbf{J}$ are the sensitivity functions given in equation (14).

The stability of the inversion is largely controlled by requiring the conductivity to vary smoothly. Larger values of λ result in smooth and stable solutions at the expense of resolution. It even allows for the solution of grossly underdetermined problems (Tikhonov and Arsenin, 1977). In this single-hole inversion study, the parameter λ is progressively selected in the inversion process. The selection procedure starts with executing a given number of inversions using nl different multipliers that are spaced appropriately. The same Jacobian is used at this step. As a result nl updated parameter sets are produced, followed by nl forward model calculations resulting in nl data misfits. Among these, the model and parameter λ giving the lowest data misfit are chosen for optimum ones. In this selection scheme, the IE modeling is quite attractive in speed because Green's functions, the most time consuming part in IE methods, are repeatedly re-usable throughout the selection procedure.

The conductivity model shown on the left of Figure 6 is chosen to evaluate the performance of extended Born inversion using the LN approximation. The model consists of two cylindrically symmetric bodies, one conductive (1 S/m) and the other resistive (0.01 S/m), in a whole space of 0.1 S/m. A FE scheme (Lee *et al.*, 2002) is used to generate synthetic data. The accuracy of the FE scheme is estimated as a level of less than 1%. Using a vertical magnetic dipole as a source, vertical magnetic fields are computed at five source-receiver offsets of 4 m through 8 m at three frequencies of 12 kHz, 24 kHz and 42 kHz. Using 3-digit synthetic data generated by the FE method, the inversion is started with an initial model of 0.25 S/m uniform whole space. In this test, $nl = 3$ is used in each iteration to select parameter update and Lagrange multiplier.

After 6 iterations, the two bodies are clearly reconstructed as shown on the right of Figure 6. The recovered conductivity is found to be nearly the same in the conductive body but is overestimated in the resistive body. The inversion process is quite stable as shown in Figure 7, where the rms misfit decreases from the initial guess of 0.478 (not shown in Figure 7) to under 0.01 after 6 iterations. The rms misfit of 0.01 is assumed to be a target misfit level because the error level in the synthetic responses is estimated to be

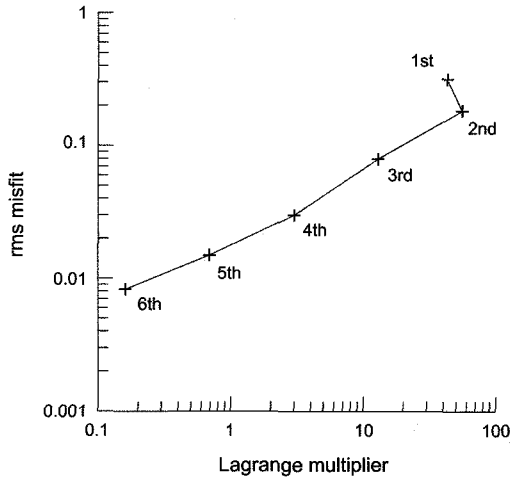

Fig. 7. Convergence in rms misfit for the synthetic model inversion.

about 1%. Also, the smoothing parameter varies significantly during the inversion process. This means it is difficult to determine the parameter a priori.

Conclusions

The extended Born or LN approximation of IE solution has been applied to inverting single-hole EM data using a cylindrically symmetric model. The extended Born approximation is less accurate than a full solution but much superior to the simple Born approximation. Moreover, when applied to the cylindrically symmetric model with a vertical magnetic dipole source, the accuracy of LN approximation is greatly improved because electric fields are scalar and continuous everywhere. One of the most important steps in the inversion is the selection of a proper regularization parameter for stability. The LN solution provides an efficient means for selecting an optimum regularization parameter, because Green's functions, the most time consuming part in IE methods, are repeatedly re-usable at each iteration. In addition, the IE formulation readily contains a sensitivity matrix, which can be revised at each iteration at little expense. In this paper, a fast inversion scheme has been developed to analyze EM fields obtained in a single-hole environment, and tested to show its stability and effectiveness using synthetic data.

Acknowledgments

This research was supported by Korea Research Foundation (KRF-2000-015-DP0431). This work is conducted as a part of the joint research between Research Institute of Environmental Geosciences, Pukyong National University, Korea and National Research Institute of Agricultural Engineering, Japan.

References

Alumbaugh, D. L., and Morrison, H. F., 1995, Theoretical and practical considerations for crosswell electromagnetic tomography assuming a cylindrical geometry: *Geophysics*, **60**, 846-870.

Alumbaugh, D. L., and Newman, G. A., 1997, Three-dimensional massively parallel electromagnetic inversion-II. Analysis of crosswell electromagnetic experiment: *Geophys. J. Int.*, 128, 355-363.

Habashy, T. M., Groom, R. M., and Spies, B. R., 1993, Beyond the Born and Rytov approximations: a nonlinear approach to electromagnetic scattering: *J. Geophys. Res.*, **98**, 1795-1775.

Hohmann, G. W., 1975, Three-dimensional induced polarization and EM modeling: *Geophysics*, **40**, 309-324.

Hohmann, G. W., 1988, Numerical modeling for electromagnetic methods of geophysics, in Nabighian, M. N., Ed., Electromagnetic methods in applied geophysics, Vol. 1: *Soc. Expl. Geophys.*, 313-363.

Lee, K. H., Kim, H. J., and Uchida, T., 2002, Electromagnetic fields in steel-cased borehole: *Geophys. Prosp.* (submitted)

Newman, G. A., 1995, Crosswell electromagnetic inversion using integral and differential equations: *Geophysics*, **60**, 899-911.

Raiche, A. P., 1974, An integral equation approach to 3D modeling: *Geophys. J. Roy. astr. Soc.*, **36**, 363-376.

Sena, A. G., and Toksoz, M. N., 1990, Simultaneous reconstruction of permittivity and conductivity for crosshole geometries: *Geophysics*, **55**, 1302-1311.

Tikhonov, A. N., and Arsenin, V. Y., 1977, Solutions to Ill-Posed Problems: John Wiley and Sons, Inc.

Ward, S. H., and Hohmann, G. W., 1988, Electromagnetic Theory for Geophysical Applications, in Nabighian, M. N., Ed., Electromagnetic methods in applied geophysics, Vol. 1: *Soc. Expl. Geophys.*, 131-312.

Wilt, M. J., Alumbaugh, D. L., Morrison, H. F., Becker, A., Lee, K. H., and Deszcz-Pan, M., 1995, Crosshole electromagnetic tomography: System design considerations and field results: *Geophysics*, **60**, 871-885.

Zhdanov, M. S., and Fang, S., 1996, Quasi-linear approximation in 3-D EM modeling: *Geophysics*, **61**, 646-665.

Zhou, Q., Becker, A., and Morrison, H. F., 1993, Audio-frequency electromagnetic tomography in 2-D: *Geophysics*, **58**, 482-495.